J. Marine. Sci. Appl. (2008) 7:82-90
DOI: 10.1007/s11804-008-7071-3

Dynamic plastic response of clamped stiffened plates with large deflection

PENG Ying* (彭　英), **YANG Ping** (杨　平)

School of Transportation, Wuhan University of Technology, Wuhan 430063, China

Abstract: Study on the dynamic response, and especially the nonlinear dynamic response of stiffened plates is complicated by their discontinuity and inhomogeneity. The finite element method (FEM) and the finite strip method are usually adopted in their analysis. Although many useful conclusions have been obtained, the computational cost is enormous. Based on some assumptions, the dynamic plastic response of clamped stiffened plates with large deflections was theoretically investigated herein by a singly symmetric beam model. Firstly, the deflection conditions that a plastic string must satisfy were obtained by the linearized moment-axial force interaction curve for singly symmetric cross sections and the associated plastic flow rule. Secondly, the possible motion mechanisms of the beam under different load intensity were analysed in detail. For structures with plastic deformations, a simplified method was then given that the arbitrary impact load can be replaced equivalently by a rectangular pulse. Finally, to confirm the validity of the proposed method, the dynamic plastic response of a one-way stiffened plate with four fully clamped edges was calculated. The theoretical results were in good agreement with those of FEM. It indicates that the present calculation model is easy and feasible, and the equivalent substitution of load almost has no influence on the final deflection.

Keywords: dynamic plastic response; stiffened plates; large deflection; singly symmetric cross section
CLC number: TU311.3　**Document code:** A　**Article ID:** 1671-9433(2008)02-0082-09

1 Introduction

Stiffened plates have wide applications in civil engineering, aerospace and marine structures. The investigation on the dynamic inelastic response of stiffened plates under high intensity pulse has received much attention of many engineers and scholars. Houlston et al.[1-2] analyzed the dynamic response of Adina and the finite strip method. Olson[3] summarized the efficient model of blast loaded stiffened plate and cylindrical shell structures, and satisfactory results were obtained by calculating some examples with different models. In China, the dynamic plastic responses of fully clamped square stiffened plates and a stiffened plate construction with one longitudinal stiffener and many equally spaced transverse stiffeners subjected to blast loading were analyzed by Liu et al.[4-5] using the principle of virtual work and the rigid-perfectly plastic constitutive model.

The dynamic plastic response of clamped stiffened plates with large deflection subjected to high intensity pulse is studied theoretically with a beam model that has a singly symmetric cross section in this paper.

2 Theoretical model and mechanisms of deformation

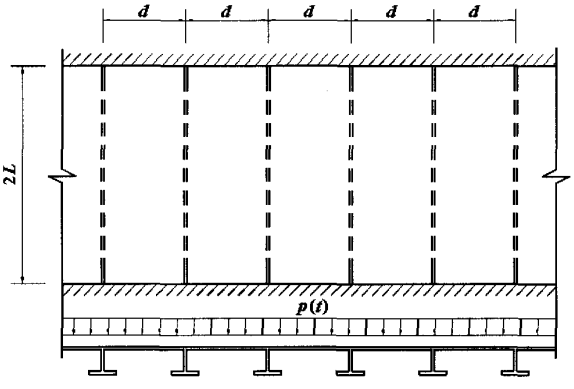

Fig.1 Stiffened plate subjected to uniformly distributed pressure pulse

A stiffened plate spanning a distance of $2L$ with uniform stiffener spacing d is considered (Fig.1). The longitudinal edges of the stiffened plate are fully clamped. The plate is subjected to a suddenly applied,

Received date: 2007-07-25.
***Corresponding author E-mail:** mypinpin@163.com

uniformly distributed load $p(t)$. Such a beam model with singly symmetric cross section is used to replace the stiffened plate in theoretical analysis that one-half of the distance to each neighboring stiffener is taken as the effective breadth, and the uniformly distributed pressure pulse applies through the beam's axis of symmetry, as shown in Fig.2(a).

The present study is based on the following assumptions:

1) The plate and stiffeners are made of isotropic, rigid-perfectly plastic material, neglecting the effects of elasticity and strain rate.

2) Shear deformation and rotary inertia effects are ignored.

3) The effect of axial force on yield condition must be taken into account for the finite deflection analysis of the beam with axial constraints at both ends.

The motion of a clamped beam subjected to uniformly distributed pressure pulse is assumed to proceed under the following three different mechanisms depending on the impact load intensity and the beam deflection:

1) The deflected shape of the beam consists of stationary plastic hinges locating at the supports and the mid-span with two rigid connecting pieces. This deformation mechanism is referred to as the mid-span hinge mechanism, as shown in Fig.2(b).

2) The deflected shape of the beam consists of stationary plastic hinges locating at the supports and two traveling plastic hinges at some distance $X(t)$ to either side of the mid-span, as shown in Fig.2(c). The hinges located inside the beam span will move towards or outwards the centre as the motion proceeds depending on the change of pressure pulse. This mode of response is referred to as the traveling hinge mechanism.

3) As the motion continues and the deflection increases, the axial force in the beam increases but the bending moment resistance decreases. When the entire beam section yields in tension, the beam has no stiffness to resist moments. Then the beam responds as a plastic string with a constant tension. This mechanism is thus referred to as the string mode (Fig.2(d)).

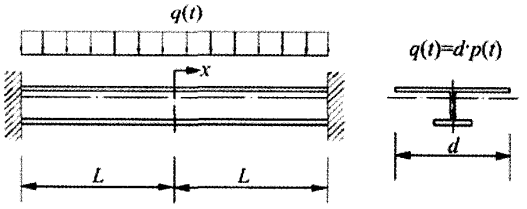

(a) Beam model

(b) Beam mechanism 1

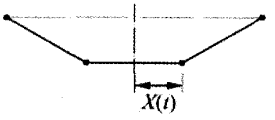

(c) Beam mechanism 2

(d) String mode

Fig.2 Beam model and mechanisms of deformation

3 The bending moment-axial force interaction relation

In the dynamic plastic response analysis of the axially constrained beams with large deflection, the axial force can't be ignored with the extension of centroidal axis when the deflection reaches the magnitude of the beam height. The effect of axial force on yield condition must be taken into account, so the bending moment-axial force interaction relation should be used in the analysis.

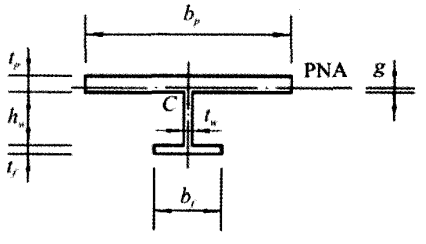

Fig.3 Cross section of a singly symmetric I-beam

The interaction relation between axial force N and bending moment M for singly symmetric cross sections should be determined by the given cross section if the neutral axis doesn't parallel the symmetric axis. For the singly symmetric I-beam section shown in Fig.3, the bending moment-axial

force interaction curve[6] is shown in Fig.4(a). It's very difficult to utilize the interaction curve due to its nonlinearity, so the linearized curve by an inner polygon is used to simplify the calculation, as shown in Fig.4(b).

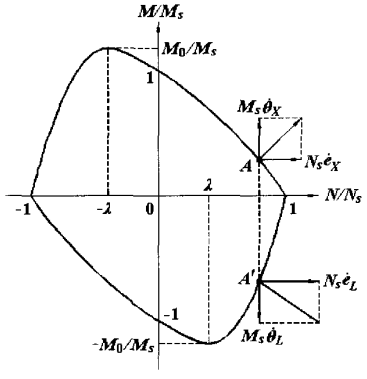

(a) Actual interaction curves

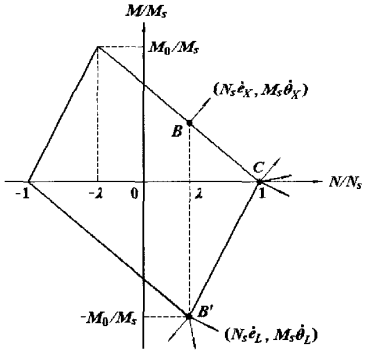

(b) Linearized interaction curves

Fig.4 Interaction curves for a singly symmetric I-beam

Suppose that axial force is positive in tension and bending moment is positive if the outer fiber of the flange is in tension. The ultimate axial force is N_s. If there's no axial force in the cross section, the ultimate bending moment will be M_s. The plastic neutral axis(PNA) will offset from the initial position if there're both bending moment and axial force in the cross section. As the neutral axis coincides with the centroidal axis, the ultimate moment M_0 occurs at the supports, resulting in an axial force of magnitude λN_s. By the principle of virtual work, the static ultimate load q_0 is obtained as

$$q_0 = \frac{2(M_X - M_L)}{L^2} = \frac{4M_0}{(1+\lambda)L^2}, \tag{1}$$

where the subscripts X and L denote variables at the traveling hinges ($x=\pm X$) and the support hinges ($x=\pm L$), respectively.

The plastic hinges formed by bending moment and axial force are defined as the generalized plastic hinges. There're both extensional strain rate and curvature strain rate at the generalized plastic hinges. The plastic deformation vector ($N_s\dot{e}, M_s\dot{\theta}$) of a hinge must be outwardly normal to the yield curve at the considered stress state according to the associated plastic flow rule. Because of the kinematic constraints, stress states can only exist at points of slope discontinuity of the approximate yield curve, for at these points the deformation ratios can lie within a range of values, as indicated in Fig.4(b). Immediately at the onset of finite displacements, the stress states will correspond to points B and B' at the traveling and support hinges, respectively, and the hinge mechanism response occurs[7] when

$$0 \le W \le W_s, \tag{2}$$

where $W_s = \dfrac{2M_0}{N_s(1-\lambda^2)}$ is the occurred critical displacement of a plastic string. For displacement outside this range, the stress states jump instantaneously to point C, and then the moment resistance is reduced to zero and the beam behaves as a plastic string under constant tension.

4 Governing equations of motion

Only one half of the beam is considered because of its symmetry. By the principle of angular momentum, the equation for dynamic equilibrium of the beam is

$$\frac{\mathrm{d}}{\mathrm{d}t}\int_0^L \bar{m}\dot{w}(L-x)\mathrm{d}x = \frac{1}{2}q(t)L^2 - (M_X - M_L + NW), \tag{3}$$

where $\bar{m}$ is the mass per unit length of the beam.

With no special indication, a triangular impact load is taken in this paper as

$$q(t) = \begin{cases} q(0)(1-t/t_d), & (0 \le t \le t_d); \\ 0, & (t > t_d). \end{cases} \tag{4}$$

4.1 Beam mechanism 1: for relatively low pulse $q_0<q(0)<3q_0$

The velocity field and the acceleration field for mechanism 1 are

$$\dot{w}(x,t)=\dot{W}(t)(1-\frac{x}{L}),\quad (0\le x\le L), \tag{5}$$

$$\ddot{w}(x,t)=\ddot{W}(t)(1-\frac{x}{L}),\quad (0\le x\le L). \tag{6}$$

1) The first phase. During this phase of motion, the entire beam is divided into two rigid pieces by the stationary plastic hinges locating at the mid-span and supports, and each rigid piece rotates round the corresponding support. Substituting Eqs.(4)~(5) for Eq.(3), and integrating it, the equation of motion for mechanism 1 is simplified as

$$\ddot{W}(t)+k^2W(t)+\frac{3}{2\bar{m}}[\frac{q(0)}{t_d}t+q_0-q(0)]=0, \tag{7}$$

where $k^2=\dfrac{3\lambda N_s}{\bar{m}L^2}$.

The solution to Eq.(7) is

$$W(t)=A_1\cos kt+A_2\sin kt+b_0t+b_1, \tag{8}$$

where $b_0=-\dfrac{3q(0)}{2\bar{m}k^2t_d}$, $b_1=\dfrac{3}{2\bar{m}k^2}[q(0)-q_0]$. The coefficients A_1 and A_2 are determined by the initial conditions $W(0)$, $\dot{W}(0)$. The motion of the beam in this phase continues until one of the following situations occurs

a) The load is removed at $t=t_d$ and the unloaded phase begins;

b) The mid-span displacement reaches W_s at $t=t_s$, and then the motion of the beam transforms into string mode from the hinge mechanism.

The string mode analysis is given in Section 4.3. Case a) will be treated in the following

2) The second phase. During this phase of motion, the beam is unloaded and the governing equation of motion (Eq.(7)) is

$$\ddot{W}(t)+k^2W(t)+\frac{3q_0}{2\bar{m}}=0. \tag{9}$$

Similarly, the mid-span displacement in this phase is obtained by Eq.(9). The beam in the second phase continues to move until

a) The beam becomes still at $t=t_f$;

b) The mid-span displacement reaches W_s at $t=t_s$.

Case a) represents a terminal situation with permanent deformation of the beam. The time t_f at which the beam becomes still can be determined by $\dot{W}(t_f)=0$, and then the final deflection of the mid-span is obtained.

4.2 Beam mechanism 2: for high pulse $q(0)>3q_0$

The velocity field and the acceleration field for mechanism 2 are

$$\dot{w}(x,t)=\begin{cases}\dot{W}(t), & 0\le x\le X(t);\\ \dot{W}(t)[\dfrac{L-x}{L-X(t)}], & X(t)<x\le L.\end{cases} \tag{10}$$

$$\ddot{w}(x,t)=\begin{cases}\ddot{W}(t), & 0\le x\le X(t);\\ [\ddot{W}(t)+\dfrac{\dot{X}(t)\dot{W}(t)}{L-X(t)}][\dfrac{L-x}{L-X(t)}], & X(t)<x\le L.\end{cases} \tag{11}$$

Substituting Eq.(10) for Eq.(3), and integrating it, the equation of motion for mechanism 2 is simplified as

$$\frac{2}{3}[\bar{m}\ddot{W}(L+2X)+\bar{m}\dot{W}\dot{X}]=q(t)(L+X)-\frac{2}{L-X}(\frac{1}{2}q_0L^2+\lambda N_sW). \tag{12}$$

The mid-span segment $0\le x\le X$ will remain flat, and the equation of motion is

$$\ddot{W}(t)=q(t)/\bar{m}. \tag{13}$$

Utilizing Eq.(13), the equation of motion [Eq.(12)] is rewritten as

$$\frac{\partial}{\partial t}[\dot{W}(L-X)^2]=\frac{3q_0L^2}{\bar{m}}+\frac{6\lambda N_s}{\bar{m}}W. \tag{14}$$

1) The first phase. During this phase, the traveling hinges will move toward the mid-span, and the outer rigid segments of the beam will increase gradually with the load decreasing for the triangular pulse. Under the initial conditions $W(0)=\dot{W}(0)=0$, the mid-span velocity and displacement can be obtained by integrating Eq.(13). Substituting them for Eq.(14), and integrating it, then the traveling hinge position in the first phase is

$$X(t)=L\left\{1-\sqrt{\frac{3q_0}{q(0)(1-\dfrac{t}{2t_d})}[1+\frac{\lambda(1+\lambda)N_sq(0)}{12\bar{m}M_0}(t^2-\frac{t^3}{4t_d})]}\right\}. \tag{15}$$

The motion of the beam in this phase continues until
a) The load is removed at $t=t_d$ and the unloaded phase begins;
b) The traveling hinges on both sides of the mid-span overlap into a single hinge at the centre of the beam at $t=t_c$. Thereafter the second phase of motion ensues and the beam deforms in accordance with mechanism 1;
c) The mid-span displacement reaches W_s at $t=t_s$, and the string response begins.

Only case a) will be studied in the following to shorten the length of this paper.

2) The second phase. During this phase of motion, the beam is unloaded and the traveling hinges continue to move toward the mid-span. Within the flat central segment $0\le x\le X$, the shear at $\pm X$ must be zero with $q(t)=0$, and then the governing equation of motion (Eq.(13)) becomes

$$\ddot{W}(t)=0,\quad 0\le x\le X(t). \tag{16}$$

The flat central segment moves with a constant velocity according to Eq.(16). Integrating it, and making use of the initial conditions $\dot{W}(t_d)$, $W(t_d)$, the mid-span velocity and displacement in the second phase can be easily obtained. The initial traveling hinge position $X(t_d)$ in this phase is obtained from Eq.(15). Integrating Eq.(14) from t_d to t, the traveling hinge position in the second phase can be given as

$$X(t)=L-\{[L-X(t_d)]^2+\frac{3}{\bar{m}}[\frac{q_0L^2}{\dot{W}(t_d)}+\frac{2\lambda N_sW(t_d)}{\dot{W}(t_d)}-2\lambda N_st_d](t-t_d)+\frac{3\lambda N_s}{\bar{m}}(t^2-t_d^2)\}^{1/2}. \tag{17}$$

The motion of the beam in the second phase will continue until
a) The width of the flat central segment continues to shorten until $t=t_c$, the traveling hinges overlap into a single hinge at the beam centre. Thereafter the third phase of motion ensues and the beam deforms in accordance with mechanism 1;
b) The mid-span displacement reaches W_s at $t=t_s$, and the string response begins.

Case a) will be treated in the following.

3) The third phase. During this phase of motion, the beam is unloaded and deformed by mechanism 1. The time t_c can be determined by Eq.(17) with $X(t_c)=0$. The method of analysis for the third phase is similar to Section 4.1. The motion of the beam in the third phase continues until
a) The beam becomes still at $t=t_f$;
b) The mid-span displacement reaches W_s at $t=t_s$.

4.3 String mode: for the mid-span displacement $W\ge W_s$

Whether the string mode occurs does not depend on the overlap of the traveling hinges, but on the deflection of the beam. When the mid-span displacement reaches W_s at $t=t_s$, the motion of the beam transforms into string mode from the hinge mechanism. The deformed beam profile in plastic string mode can be represented by

$$w(x,t)=W(t)\cos\frac{\pi x}{2L}. \tag{18}$$

The mid-span displacement W and the kinetic energy of the beam at time t_s are held constant through the sudden change in the deformation mode[7]. Denoting the mid-span velocity at an instant before $t=t_s$ as $\dot{W}(t_s^-)$ and at an instant after as $\dot{W}(t_s^+)$, for beam mechanism 2, the relation between them is given by equating the kinetic energy through the transition as

$$\dot{W}(t_s^+)=\dot{W}(t_s^-)\sqrt{\frac{2}{3}[1+\frac{2X(t_s^-)}{L}]}, \tag{19}$$

and for beam mechanism 1, the relation between $\dot{W}(t_s^+)$ and $\dot{W}(t_s^-)$ can be obtained from Eq.(19) with $X(t_s^-)=0$ as the beam changes its deformation mode at time t_s.

1) Loaded string mode. In this case, the beam responds as a plastic string until the load is removed at time t_d. The equation of motion for the loaded string is

$$\bar{m}\frac{\partial^2w}{\partial t^2}-N_s\frac{\partial^2w}{\partial x^2}=q(t). \tag{20}$$

Under the boundary conditions $w(\pm L,\ t)=0$, the displacement field of the beam can be represented by a Fourier series as $w(x,t)=\sum_{n=1,3,5,\cdots}^{\infty}W_n(t)\cos\frac{n\pi x}{2L}$, and the load $q(t)$ is also represented by the same mode shape function with $w(x,\ t)$. By substituting $w(x,\ t)$ and $q(t)$ for Eq.(20), and taking only the first term, a simple equation of motion is obtained as

$$\ddot{W}(t)+\frac{\pi^2 N_s}{4\bar{m}L^2}W(t)=\frac{4q(0)}{\pi\bar{m}}(1-\frac{t}{t_d}). \quad (21)$$

By introducing $k'^2=\frac{\pi^2 N_s}{4\bar{m}L^2}$, the solution to Eq.(21) is similar to that of Eq.(7).

2) Unloaded string phase. During this phase, the beam also responds as a plastic string until it becomes still. The equation of motion [Eq.(21)] for the unloaded string is

$$\ddot{W}(t)+k'^2W(t)=0. \quad (22)$$

The mid-span displacement during this phase can be easily obtained by Eq.(22). The time t_f at which the beam becomes still is also determined by $\dot{W}(t_f)=0$, and then the final deflection of the mid-span is obtained.

5 Equivalent substitution of an arbitrary impact load

It's often not realizable to know all details of arbitrary impact loads exactly in many actual engineering problems, and the analysis and calculation of them are still very difficult. So it becomes very important for us to find a simplified method that can replace the arbitrary impact loads equivalently. Based on the rigid-perfectly plastic model, Youngdahl has given a set of parameters that may be used to calculate the final plastic deformation without the effects of the pulse shape[8], as shown in Fig.5. The equivalent total impulse is defined as

$$I_{\text{eff}}=\int_{t_0}^{t_f}p(t)\mathrm{d}t, \quad (23)$$

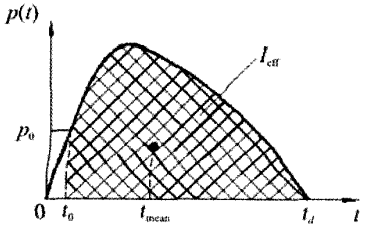

(a) Definition of p_{eff} and t_{mean}

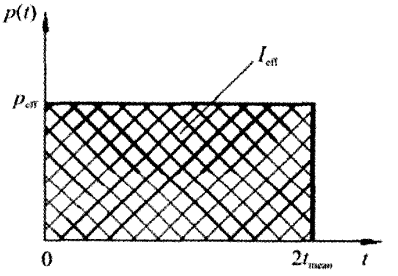

(b) Equivalent rectangular pulse

Fig.5 Youngdahl's parameters for an arbitrary impact load

where t_0 and t_f are the time when the plastic deformation commences and terminates respectively. The equivalent pulse is then defined as

$$p_{\text{eff}}=I_{\text{eff}}/2t_{\text{mean}}, \quad (24)$$

where t_{mean} corresponds to the centroid position of the effective impact load, and it is given by

$$t_{\text{mean}}=\frac{1}{I_{\text{eff}}}\int_{t_0}^{t_f}(t-t_0)p(t)\mathrm{d}t. \quad (25)$$

In Eq.(23) and Eq.(25), t_0 is taken as the time when the impact load firstly reaches the plastic ultimate load p_0. The terminative time t_f of plastic deformation is difficult to be ascertained before solving the structural response, and then it may be determined approximately by

$$I_{\text{eff}}\approx p_0(t_f-t_0). \quad (26)$$

6 Examples

The stiffened plate with four fully clamped edges in Ref.[7] is adopted to confirm the study in this paper, as shown in Fig.6. The geometry of the stiffened plate is indicated in Fig.6. The material parameters are as follows: elastic modulus E=2.07×10^{11} Pa, Poisson's ratio ν=0.3, mass density ρ=7.845×10^3 kg/m^3, static yield stress σ_s=310 MPa and effective dynamic yield stress σ_d=372 MPa. Strain rate effects are ignored in theoretical analysis, but the dynamic yield stress value is also used herein for comparison purpose. Two triangular impact loads with duration t_d=3 ms and initial load intensity $p(0)$ are considered. For the first pulse considered, $p(0)$=1.185 MPa, and for the second, $p(0)$=2.37 MPa, as shown in Fig.7(a). The equivalent rectangular pulses with duration t'_d=2 ms and constant intensity p_m=0.889 MPa and p_m=1.779 MPa, respectively, are shown in Fig.7(b).

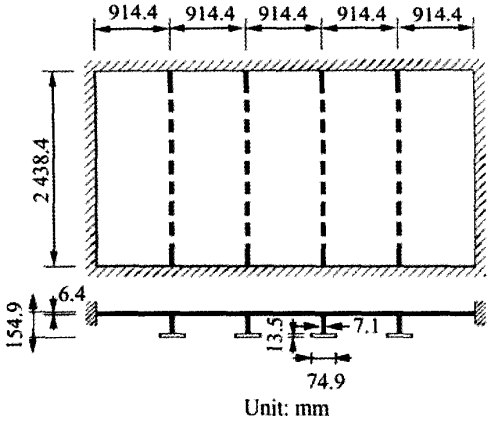

Fig.6 Geometric configuration of stiffened plate

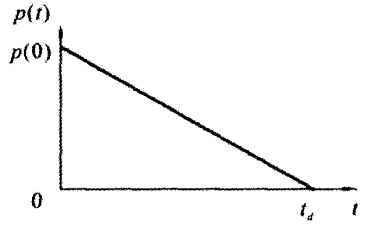

(a) Triangular impact load

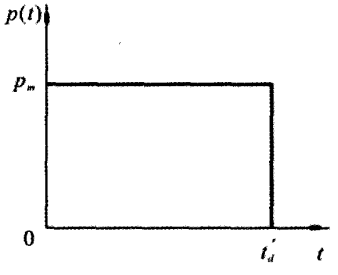

(b) Equivalent impact load

Fig.7 Impact loads

Besides theoretical calculations, the response of stiffened plate to these pulses is calculated by the FEM software Ansys using the beam model and by the FEM software Abaqus/Explicit using the whole stiffened plate model. The rigid-perfectly plastic material model is adopted in theoretical analysis, but the effects of elasticity are considered in FEM calculations. The theoretical and FEM results are compared herein. The mid-span displacement $W(t)$ and the traveling hinge position $X(t)$ under triangular impact loads are plotted in Figs.8~9, respectively.

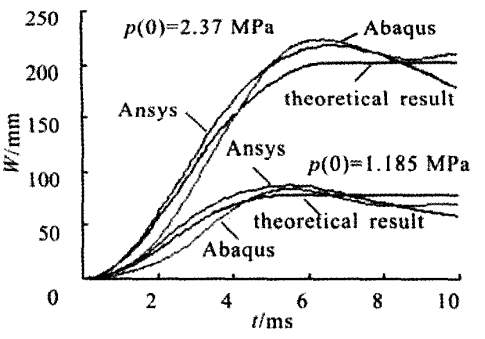

Fig.8 Mid-span displacement response of the stiffened plate under triangular impact loads

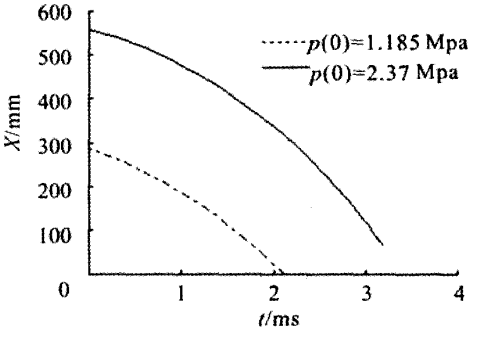

Fig.9 Positions of the traveling hinges under triangular impact loads

The theoretical and FEM results are in good agreement as seen from Fig.8, which shows that the basic assumptions and approximations for simplifying calculations are reasonable and the beam model in theoretical analysis is adoptable. It should be indicated that owing to the presence of elasticity, the stiffened plate does not become still but oscillates about some average value when the mid-span displacement reaches the maximum value in FEM calculations. Fig.8 also shows that the final displacement of the triangular pulse with $p(0)$=1.185 MPa is less than that required for string response. However, larger displacement is induced and a significant amount of string response occurs for the pulse with $p(0)$=2.37 MPa.

It can be seen from Fig.9 that for the triangular pulse with initial intensity $p(0)$=1.185 MPa, the two traveling hinges have overlapped into a single hinge at the beam centre before the load is removed. However, for the pulse with initial intensity $p(0)$=2.37 MPa, the two traveling hinges continue to move towards the beam centre after the load is removed until the beam

deflection becomes sufficiently large to initiate the string mode, but they still haven't met.

To confirm the validity of equivalent substitution, the mid-span displacement $W(t)$ and the traveling hinge position $X(t)$ under triangular impact loads and equivalent rectangular pulses are plotted in Figs.10~11, respectively.

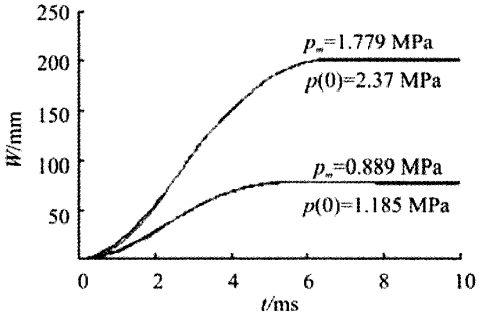

(a) Theoretical results

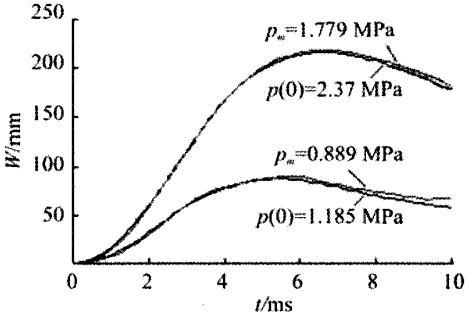

(b) Results of Ansys

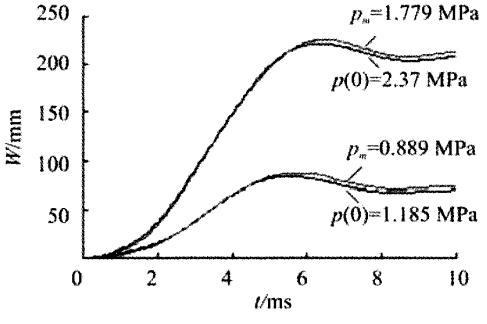

(c) Results of Abaqus/Explicit

Fig.10 Mid-span displacement responses

In theoretical and FEM calculations, the responses under equivalent rectangular pulses and triangular impact loads are in very close agreement, with the equivalent rectangular pulse prediction slightly higher than the triangular pulse's, that is to say, the equivalent substitution of impact loads almost has no influence on the mid-span displacement, as shown in Figs.10(a)~(c). Therefore, the equivalent substitution method of arbitrary impact loads can be used to simplify the calculation if we only want to know the structural displacement responses.

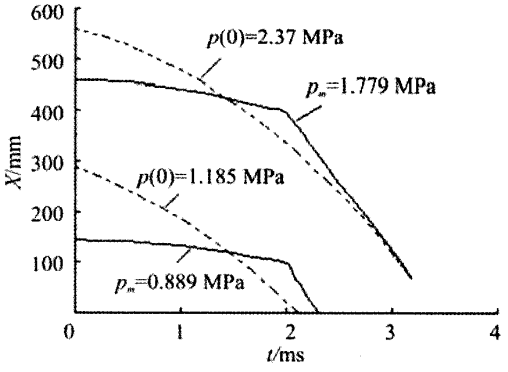

Fig.11 Positions of the traveling hinges

The positions of the traveling hinges are changed obviously if triangular impact loads are replaced by rectangular pulses equivalently, as seen in Fig.11. For equivalent rectangular pulses, the two traveling hinges continue to move towards the beam centre after the loads are removed. They will overlap into a single hinge at some time for the pulse of intensity p_m=0.889 MPa. However, they still haven't met as the beam deflection becomes sufficiently large to initiate the string mode for the pulse of intensity p_m=1.779 MPa. The beam undergoes the same mechanisms of motion for the equivalent rectangular pulse with intensity p_m=1.779 MPa and the triangular pulse with initial intensity $p(0)$=2.37 MPa.

7 Conclusions

The dynamic plastic response of clamped stiffened plates with large deflection subjected to high intensity pulse is studied theoretically by a beam model with singly symmetric cross section in this paper. For comparison purpose, the one-way stiffened plate with four fully clamped edges in Ref.[7] is used to calculate the response. It indicates that the theoretical results are in good agreement with those from FEM and Ref.[7], and then the reasonability of some basic assumptions, approximations and the beam model in

theoretical analysis is confirmed. Moreover, for plastic deformation structures, replacing arbitrary impact loads by equivalent rectangular pulses almost has no influence on the final deflection.

References

[1] HOULSTON R, DESROCHERS C G. Nonlinear structural response of ship panels subjected to air blast loading[J]. Computers & Structures, 1987, 26(1/2): 1-15.

[2] HOULSTON R. Finite strip analysis of plates and stiffened panels subjected to air-blast loads[J]. Computers & Structures, 1989, 32(3-4): 647-659.

[3] OLSON M D. Efficient modeling of blast loaded stiffened plate and cylindrical shell structures[J]. Computers & Structures, 1991, 40(5): 1139-1149.

[4] LIU T G, HU Y W, ZHENG J J. Dynamic response analysis of rigid perfectly plastic clamped square plates with stiffener subjected to blast loading[J]. Explosion and Shock Waves, 1994, 14(1): 55-65(in Chinese).

[5] LIU T G, TANG W Y. The dynamic plastic response of a structure with stiffened plates under impulsive loading[J]. J Huazhong Univ of Sci & Tech, 1996, 24(1): 106-109(in Chinese).

[6] PENG Y. Research on nonlinear dynamic response and buckling of stiffened plates under impact loading[D]. Wuhan: Wuhan University of Technology, 2007(in Chinese).

[7] SCHUBAK R B, OLSON M D, ANDERSON D L. Rigid-plastic modeling of blast-loaded stiffened plates-Part I: One-way stiffened plates[J]. Int J Mech Sci, 1993, 35(3-4): 289-306.

[8] YU T X, STRONGE W J. Dynamic Models for Structural Plasticity[M]. Beijing: Peking University Press, 2002: 122-123(in Chinese).

PENG Ying was born in 1980. She is a candidate for doctor's degree at Wuhan University of Technology. Her current research interests include dynamic stability of structures, computation mechanics, etc.

Dynamic plastic response of clamped stiffened plates with large deflection

作者： PENG Ying， YANG Ping
作者单位： School of Transportation, Wuhan University of Technology, Wuhan 430063, China
刊名： 船舶与海洋工程学报
英文刊名： JOURNAL OF MARINE SCIENCE AND APPLICATION
年，卷(期)： 2008，7(2)
引用次数： 0次

参考文献(8条)

1. HOULSTON R. DESROCHERS C G Nonlinear structural response of ship panels subjected to air blast loading 1987(1-2)

2. HOULSTON R Finite strip analysis of plates and stiffened panels subjected to air-blast loads 1989(3-4)

3. OLSON M D Efficient modeling of blast loaded stiffened plate and cylindrical shell structures 1991(05)

4. LIU T G. HU Y W. ZHENG J J Dynamic response analysis of rigid perfectly plastic clamped square plates with stiffener subjected to blast loading 1994(01)

5. LIU T G. TANG W Y The dynamic plastic response of a structure with stiffened plates under impulsive loading 1996(01)

6. PENG Y Research on nonlinear dynamic response and buckling of stiffened plates under impact loading 2007

7. SCHUBAK R B. OLSON M D. ANDERSON D L Rigid-plastic modeling of hlast-loaded stiffened plates-Part I:One-way stiffened plates 1993(3-4)

8. YU T X. STRONGE W J Dynamic Models for Structural Plasticity 2002

相似文献(2条)

1. 会议论文 PENG Ying. YANG Ping Dynamic Plastic Response of Stiffened Plates under Explosion Pressure 2007

The dynamic plastic response of stiffened plates under explosion pressure is theoretically investigated in this paper. The possible motion mechanisms of the beam under different load intensity are analysed in detail, and the relevant criteria are given. Moreover, the simplified method is presented that the arbitrary impact load can be replaced equivalently by a rectangular pulse. To confirm the validity of present method, the dynamic plastic response of a one-way stiffened plate with four fully clamped edges is calculated. It indicates that the present method is easy and feasible for ship structural design.

2. 期刊论文 彭英. 杨平. PENG Ying. YANG Ping 加筋板的大挠度塑性动力响应研究 -舰船科学技术2008, 30(1)

对加筋板的大挠度塑性动力响应进行了理论研究,应用单轴对称截面的线性化轴力-弯矩交互作用曲线和相关联的塑性流动法则推出了梁达到塑性弦状态所应满足的挠度条件.此外,详细地分析了梁在不同载荷情况下可能的运动模式.最后应用本文理论和有限元软件ANSYS、ABAQUS/Explicit对四边固支单向加筋板结构进行了求解.